



ORIGINAL ARTICLE

Differential reactivity of SARS-CoV-2 S-protein T-cell epitopes in vaccinated versus naturally infected individuals

Daniel J Browne¹ , Pauline Crooks², Corey Smith^{2,3}  & Denise L Doolan^{1,4}

1 Centre for Molecular Therapeutics, Australian Institute of Tropical Health and Medicine, James Cook University, Cairns, QLD, Australia

2 QIMR Berghofer Centre for Immunotherapy and Vaccine Development and Translational and Human Immunology Laboratory, Department of Immunology, QIMR Berghofer Medical Research Institute, Brisbane, QLD, Australia

3 Faculty of Medicine, The University of Queensland, Brisbane, QLD, Australia

4 Institute for Molecular Bioscience, The University of Queensland, St Lucia, QLD, Australia

Correspondence

DL Doolan, Institute for Molecular Bioscience, The University of Queensland, St Lucia, QLD, Australia.

E-mail: d.doolan@imb.uq.edu.au

Received 18 November 2024;

Revised 20 February and 14 March 2025;

Accepted 18 March 2025

doi: 10.1002/cti2.70031

Clinical & Translational Immunology

2025; 14: e70031

Abstract

Objectives. Vaccine-induced protective immunity against SARS-CoV-2 has proved difficult to sustain. Robust T-cell responses are thought to play an important role, but T-cell responses against the SARS-CoV-2 spike protein (S-protein), the core vaccine antigen, following vaccination or natural infection are incompletely understood. **Methods.** Herein, the reactivity of 170 putative SARS-CoV-2 S-protein CD8⁺ and CD4⁺ T-cell peptide epitopes in the same individuals prior to vaccination, after COVID-19 vaccination, and again following subsequent natural infection was assayed using a high-throughput reverse transcription-quantitative PCR (HTS-RT-qPCR) assay. **Results.** The profile of immunoreactive SARS-CoV-2 S-protein epitopes differed between vaccination and natural infection. Vaccine-induced immunoreactive epitopes were localised primarily into two extra-domainal regions. In contrast, epitopes recognised following natural infection were spread across the antigen. Furthermore, T-cell epitopes in naïve individuals were primarily recognised in association with HLA-A, while natural infection shifted epitope associations towards HLA-B, particularly the B7 supertype. **Conclusion.** This study provides insight into T-cell responses against the SARS-CoV-2 S-protein following vaccination and subsequent natural infection.

Keywords: COVID-19 vaccines, HLA-B7 antigen, SARS-CoV-2, spike glycoprotein, T-cell epitopes, T-lymphocyte

INTRODUCTION

The SARS-CoV-2 coronavirus, the causative agent of COVID-19,¹ is now endemic throughout the world, despite the rapid development of effective vaccines that induce robust immunity against the

virus.² While vaccination against SARS-CoV-2 has substantially reduced the mortality and morbidity associated with COVID-19,^{3–5} the effectiveness of the available vaccines decreases relatively rapidly,^{6,7} and multiple novel viral variants have emerged that can evade vaccine-induced

protection.⁸ By 2023, individuals who received the original wild-type COVID-19 vaccines were found to have minimal protection against severe disease requiring hospital admission.⁹ This waning immunity contrasts with the sustained protection provided by many vaccines included in global adolescent immunisation schedules, such as measles, mumps, rubella and hepatitis B.^{10,11} Following convalescence from exposure to SARS-CoV-2, natural immunity provides robust protection against reinfection and COVID-19-related hospitalisation, with this protection remaining relatively high over a longer period than vaccination.^{12–15} Indeed, hybrid immunity, resulting from vaccination followed by subsequent natural infection, appears to provide the highest level of protection.¹⁵

Many COVID-19 vaccines, including the Pfizer-BioNTech mRNA vaccine (BNT162b2) and the Moderna mRNA vaccine (mRNA-1273), were intended to induce high levels of neutralising antibodies.¹⁶ Conversely, the AstraZeneca vaccine (ChAdOx1 nCoV-19) was designed to induce a balanced immune response that includes activated T-cell responses in addition to antibody responses.^{17,18} Both vaccine strategies proved effective at inducing robust antibody and T-cell responses, but vaccine-induced efficacy decreased relatively quickly for both.¹⁹ Promoting robust cellular immunity and cellular immune memory, particularly T-cell-mediated immunity, is expected to enhance the development of long-term protection and maintain protection against novel viral variants.^{20–22} Broadly, CD8⁺ T cells can eliminate virally infected host cells,²³ while T helper CD4⁺ T cells play a multipurpose role, including assisting in the production of high-affinity neutralising antibodies or promoting immune activation, regulation and memory formation.²⁴ However, the specificity, magnitude and kinetics of T-cell reactivity to SARS-CoV-2 in relation to vaccination or natural infection are incompletely understood.

The magnitude of T-cell responses has been associated with the effectiveness of host immunity to SARS-CoV-2 infection.²⁵ Perturbations to T-cell populations and circulating numbers²⁶ and a decline in naïve T-cell number and diversity²⁷ have been all associated with poor COVID-19 clinical outcomes. Several HLA alleles have been identified as beneficial for immunity to SARS-CoV-2,^{15,28} while others have been found to be detrimental^{29–31} to patient outcomes.

Immunodominance is the 'choice of the immune system' to develop immunity to any specific antigen or epitope,³² and only a fraction of potential peptide epitopes induce measurable cellular immunity.³³ The tripartite interaction of expressed HLA alleles, antigen and peptide epitope chemistry, and the repertoire of available naïve T cells is the dominant paradigm that is believed to determine epitope immunodominance.³⁴ Understanding T-cell immunodominance during a SARS-CoV-2 infection following vaccination and subsequent natural infection may provide insight to develop more efficacious vaccines.

Currently, all licensed COVID-19 vaccines are based on the SARS-CoV-2 spike protein (S-protein) antigen. The S-protein is a large homotrimer transmembrane glycoprotein that facilitates SARS-CoV-2 entry by binding to the human ACE2 receptor. Each trimer consists of between 1273 and 1300 amino acids, depending on the viral variant,³⁵ which allows for a large number of potential T-cell epitopes and abundant T-cell peptide epitope–HLA presentation.³⁶ Various studies have explored S-protein epitope immunodominance or reactivity following vaccination,^{37–39} and in infected or convalescent patients.^{31,40–45} Pre-existing T-cell immunity to SARS-CoV-2 in COVID-19 naïve individuals is another notable phenomenon observed during the COVID-19 pandemic,^{41,46} pre-existing presumably from exposure to other endemic coronaviruses.⁴⁷ Further developing an understanding of which SARS-CoV-2 S-protein T-cell epitopes are immunodominant in pre-existing immunity, following vaccination and following an infection may provide critical insight for future vaccine design.

The identification of immunodominant T-cell epitopes within the SARS-CoV-2 S-protein involves analysis of peptide-stimulation reactivity by human peripheral blood mononuclear cells (PBMCs), quantified by measuring markers of activation, such as the secretion of interferon gamma (IFN- γ).⁴⁸ T-cell epitopes can be identified by screening large panels of overlapping peptides representing the complete protein or a more focused panel of putative peptide epitopes predicted using software, such as the T-cell epitope NetMHCpan HLA-peptide-binding prediction tool⁴⁹ within the Immune Epitope Database (IEDB).⁵⁰ In this study, 170 CD8⁺ and CD4⁺ T-cell peptide epitopes were identified from

the SARS-CoV-2 S-protein, based on prediction to bind with high affinity to a range of class I and class II HLA alleles using the IEDB NetMHCpan algorithm. Thousands of peptides were identified overall and were subsequently prioritised by reported immunogenicity^{21,41,43,46,51,52} (as well as HLA-peptide binding affinity) to define a subset of putative T-cell epitopes for study.

Peptide epitopes are typically screened for immunoreactivity with conventional assays, including IFN- γ ELISpot, intracellular cytokine staining (ICS) or activation-induced marker (AIM) assay.^{53–55} These assays typically require a high number of PBMCs, especially when screening the large number of potential peptide epitopes available within the SARS-CoV-2 S-protein. To address this limitation, we developed a sensitive and specific high-throughput screening reverse transcription-quantitative PCR (HTS-RT-qPCR) assay to screen large panels of putative T-cell epitope peptides from low numbers of PBMCs.⁵⁶ Herein, we applied this assay to identify immunoreactive T-cell epitopes from SARS-CoV-2 recognised by humans naïve to SARS-CoV-2 (pre-existing immunity, cross-reactive to other viruses), following COVID vaccination and following SARS-CoV-2 infection. We used our HTS-RT-qPCR assay to evaluate the immunoreactivity of these peptide epitopes in donors either naïve to the S-protein, vaccinated with the S-protein or following a subsequent natural infection. Where available, matched PBMCs collected from donors' pre-exposure, post-vaccination and post-infection were tested. This study contributes to the understanding of vaccine epitope immunodominance and kinetics, while highlighting the utility of HTS-RT-qPCR for peptide epitope immunoreactivity testing.

RESULTS

All donors developed S-protein-specific antibodies but, as expected, none produced nucleocapsid-specific antibodies after receiving the S-protein-based SARS-CoV-2 vaccine

Following vaccination and subsequent natural infection, SARS-CoV-2 S-protein antibody titres increased in all donors, except Donor 3 (Supplementary figure 1). Antibody titres specific to the NCAP remained low after vaccination and rose only upon infection in all donors except for Donor 3, whose NCAP titres stayed low

(Supplementary figure 1). These findings indicate that double homologous AstraZeneca vaccination induced robust S-protein antibody responses, and that NCAP-specific antibodies only appear after infection with SARS-CoV-2, as expected. Donor 3, despite self-reporting COVID-19, may not have been infected or failed to seroconvert.

The number of immunoreactive T-cell epitopes was generally consistent across donor immune status

We defined a list of 170 putative SARS-CoV-2 S-protein peptide epitopes (Supplementary table 1) from a total of 7500 identified CD8⁺ T-cell peptide epitope–HLA allele combinations (Supplementary figure 2); test peptides were generally restricted to either the HLA-A2, HLA-A3/11, HLA-A24, HLA-B7 or HLA-B8 MHC Class I (Supplementary figure 3) or Class II HLA-DR or HLA-DQ supertypes. These peptide epitopes were derived from the Wuhan reference strain, and analysis of sequence similarity for other SARS-CoV-2 variants was assessed and showed that the peptide epitope sequences were mostly homologous to clinically relevant circulating SARS-CoV-2 variants but not homologous to other circulating coronaviruses (Supplementary figure 4). Peptides were prioritised firstly by the sum of the response as identified from Tarke *et al.*,⁴³ then by their IEDB predicted binding score (Supplementary table 1).

To study the magnitude and kinetics of T-cell reactivity to these peptide epitopes in pre-vaccinated, post-vaccinated and post-SARS-CoV-2 infected individuals, we used our published HTS-RT-qPCR assay⁵⁶ to determine the expression of IFN- γ mRNA from PBMCs stimulated with these peptides. Defining the threshold of positivity as a doubling of IFN- γ expression ($\Delta\Delta C_t > 2$), we identified 65/170 epitopes that were immunoreactive in at least one donor. Robust T-cell epitope reactivity was identified in SARS-CoV-2 S-protein naïve individuals (17.0% positive: 29/170 epitopes, $n = 9$; Table 1), following vaccination (14.7% positive: 25/170 epitopes, $n = 10$; Table 1) and following subsequent natural exposure (16.5% positive: 28/170 epitopes, $n = 8$; Table 1), which was generally consistent with previously reported peptide immunogenicity amongst donors of similar immune status (Supplementary table 3).

No significant differences were detected in the number of positive epitopes between naïve,

Table 1. Categorical analysis of SARS-CoV-2 S-protein epitope immunoreactivity and kinetics in matched donors following vaccination and natural infection

Immunoreactive epitopes	Immune status	Positive	Negative	Total	Positive (%)	P-value vs. naïve	P-value vs. vaccination
<i>Peptide epitope immunoreactivity</i>							
Background	Naïve	29	141	170	17.0%	–	–
	Vaccinated	25	145	170	14.7%	0.6565	–
	Naturally infected	28	142	170	16.5%	> 0.9999	0.7652
						P-value vs. immune status	P-value vs. background
<i>Positive epitope kinetics</i>							
Naïve	Vaccinated	9	20	29	31.0%	–	0.0570
	Naturally infected	2	27	29	6.9%	0.0411	0.2634
Vaccinated	Naïve	9	16	25	36.0%	–	0.0330
	Naturally infected	6	19	25	24.0%	0.5380	0.3965
Naturally Infected	Naïve	2	26	28	6.9%	–	0.3997
	Vaccinated	6	22	28	24.0%	0.2516	0.2631

PBMCs ($n = 12$) were collected from donors who were either SARS-CoV-2 S-protein naïve (Naïve), following COVID-19 vaccination (Vaccinated) or following infection with SARS-CoV-2 (Naturally infected). The discovery rate of positive epitopes (% Positive) across all stimulations (Background) was determined from the relative number of reactive stimulations to non-reactive stimulations. Positive epitope kinetics tested whether positive epitopes were consistently positive across classes of immune status by comparing the discovery rate of positive epitopes to background.

vaccinated or naturally infected donors (peptide epitope immunoreactivity: $P = 0.6565$ (naïve vs. vaccinated), $P > 0.9999$ (naïve vs. naturally infected) and $P = 0.7652$ (vaccinated vs. naturally infected); Table 1). When considering individual donors, the number of reactive epitopes amongst donor-matched PBMCs was generally consistent (Figure 1a), although some significant differences were detected. Specifically, when tested with a Fisher's exact test, there was a statistically significant increase in the number of reactive epitopes between naïve and naturally infected PBMCs ($P = 0.0353$) and a decrease in the number of reactive epitopes between naïve and vaccinated PBMCs ($P = 0.0366$) from Donors 3 and 8, respectively (Supplementary table 4). Taken together, these data demonstrate that the number of immunoreactive epitopes were generally consistent across donor immune status.

High-affinity HLA-A epitopes are more immunoreactive in the naïve, while HLA-B epitopes are more immunoreactive post-natural infection

When considering the HLA supertype restriction element of the tested peptides (Figure 1b), there was no statistically significant increase in the number of reactive epitopes in HLA-matched peptides as determined by Fisher's exact test (Supplementary table 5), except for an increase in immunoreactive HLA-B7-supertype epitopes

between naïve and naturally infected PBMCs ($P = 0.0462$; Figure 1b). For epitopes predicted to bind with high affinity to any of the HLA-A gene alleles, there were no statistically significant differences in the number of immunoreactive epitopes across donor immune status by Fisher's exact testing (Supplementary table 5). However, for epitopes predicted to bind with high affinity to HLA-B gene alleles, there was a statistically significant increase in the number of immunoreactive epitopes between the naïve and the naturally infected ($P = 0.0149$; Figure 1b). Furthermore, when comparing across HLA genes, there was a statistically significant decrease in the number of immunoreactive epitopes in the naïve between HLA-A- and HLA-B-associated epitopes ($P = 0.0010$; Figure 1b). These data demonstrate that the type of epitope recognised altered from HLA-A restricted epitopes being predominantly immunoreactive in the naïve to HLA-B restricted epitopes being predominantly immunoreactive following natural infection, with a particular focus on HLA-B7 supertype epitopes.

Peptide epitopes immunoreactive following vaccination were more likely to be immunoreactive in the naïve, but not following natural infection

We examined the kinetics of epitope immunoreactivity across donor-matched naïve, vaccinated or naturally exposed samples

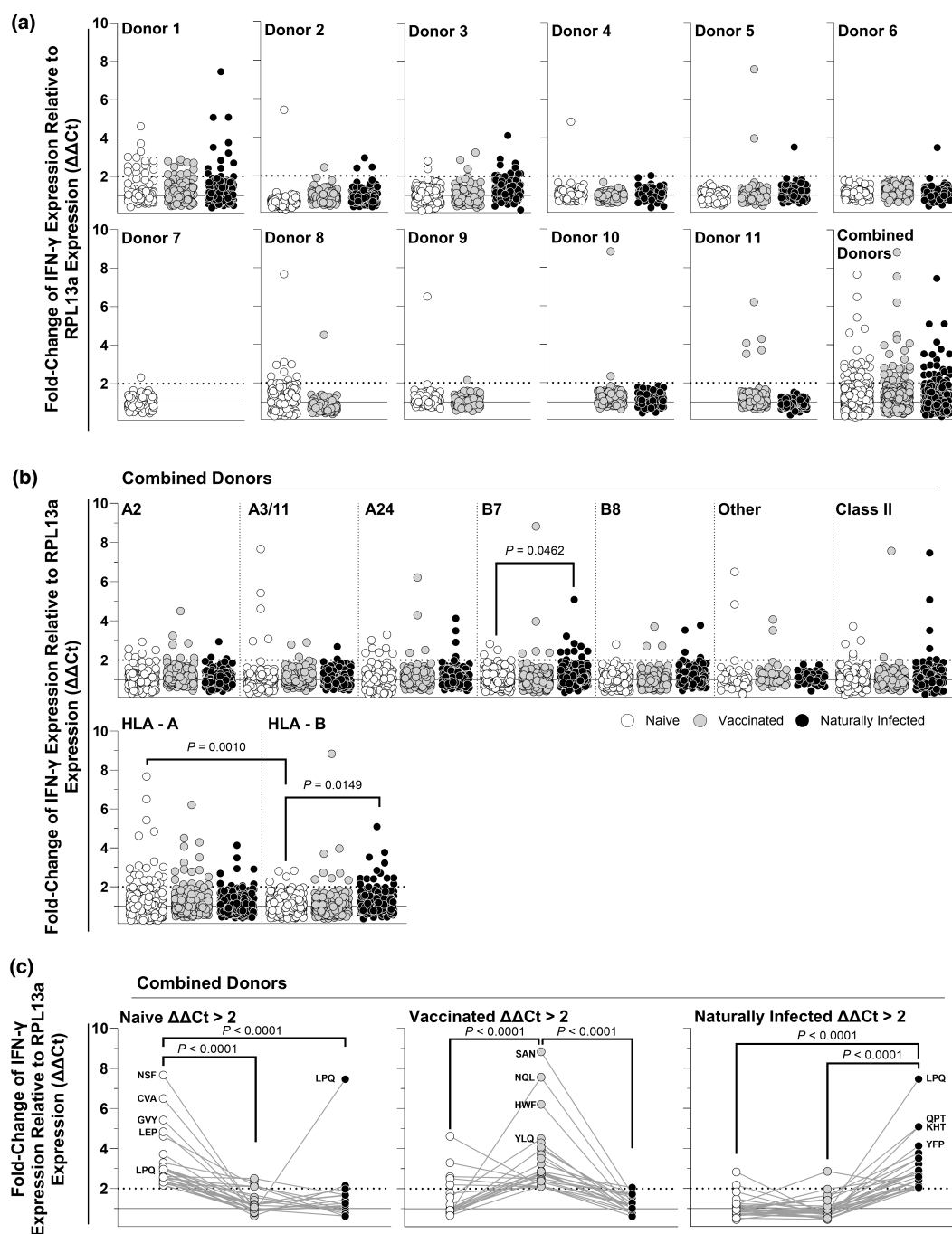


Figure 1. Peptide epitope immunoreactivity in peripheral blood mononuclear cells (PBMCs) isolated from individuals naïve to SARS-CoV-2, as well as following vaccination and natural infection. Interferon gamma (IFN- γ) expression quantified through a high-throughput RT-qPCR (HTS-RT-qPCR) assay with fold change ($\Delta\Delta Ct$) determined relative to the endogenous control reference gene Ribosomal Protein L13a (RPL13a) of PBMCs isolated from 12 individuals naïve to SARS-CoV-2 S-protein (naïve; white dots), following homologous AstraZeneca COVID-19 vaccination (vaccinated; grey dots), and following infection with SARS-CoV-2 (naturally infected; black dots) stimulated with 170 SARS-CoV-2 S-protein peptide epitopes. Shown are data sorted by donor **(a)**, sorted into HLA-A2, HLA-A3/11, HLA-A24, HLA-B7, HLA-B8, other and Class II supertype classifications **(b)**, and data showing matched peptide kinetics tracking immunoreactive epitopes ($\Delta\Delta Ct > 2$) across the naïve, vaccinated and naturally infected **(c)**. Epitopes with $\Delta\Delta Ct$ between 0 and 10 shown graphically while all data were considered for statistical analysis. Selected immunoreactive peptides shown with three-letter codes.

Table 2. Categorical analysis of immunoreactive epitope localisation within SARS-CoV-2 S-protein domains and regions following vaccination and natural infection

Domain	Immune status	Epitope in domain	Epitope outside domain	Total	In domain (%)	<i>P</i> -value vs. naïve	<i>P</i> -value vs. vaccination
NTD	Naïve	13	17	30	43.3%	–	
	Vaccinated	4	22	26	15.4%	0.0401	–
	Naturally infected	10	19	29	34.5%	0.5959	0.1302
RBD	Naïve	5	25	30	16.7%	–	
	Vaccinated	3	23	26	11.5%	0.7116	–
	Naturally infected	3	26	29	10.3%	0.7065	> 0.9999
VC1	Naïve	4	26	30	13.3%	–	
	Vaccinated	7	19	26	26.9%	0.3130	–
	Naturally infected	4	25	29	13.8%	> 0.9999	0.3153
VC2	Naïve	5	25	30	16.7%	–	
	Vaccinated	11	15	26	42.3%	0.0426	–
	Naturally infected	4	25	29	13.8%	> 0.9999	0.0321
VC1/VC2 combined	Naïve	9	21	30	30.0%	–	
	Vaccinated	18	8	26	69.2%	0.0068	–
	Naturally infected	8	21	29	27.6%	> 0.9999	0.0029

The location of immunoreactive epitopes ($\Delta\Delta C_t > 2$) was tested relative to the number of epitopes inside and outside of domains across combined ($n = 12$) donors of various immune statuses. Tested were the N-terminus domain (13–304aa; NTD), the Receptor Binding (319–541aa; RBD), Vaccination Cluster 1 (590–730aa; VC1), Vaccination Cluster 2 (905–1115aa; VC2) and epitopes within both VC1 and VC2 (Combined).

(Figure 1c). There was a statistically significant decrease ($P < 0.0001$, in all cases) in immunogenicity for epitopes that were found to be immunoreactive in the naïve (naïve $\Delta\Delta C_t > 2$), vaccinated (vaccinated $\Delta\Delta C_t > 2$) or naturally infected (naturally infected $\Delta\Delta C_t > 2$) subjects, as determined by a non-parametric Kruskal–Wallis test. Dunn's corrected multiple comparisons testing found there was a statistically significant decrease in immunogenicity at all matched kinetic timepoints ($P < 0.0001$ in all cases; Figure 1c). These data demonstrated that the immunoreactivity of epitopes varied between immune statuses.

To investigate whether there was an association between positive epitopes across immune status, we next investigated whether epitopes that were positive at one kinetic timepoint were also positive at another. Amongst the 29 epitopes identified as positive in the naïve, nine (31.0%) were also positive in the vaccinated, while two (6.9%) were positive in the naturally infected (positive epitope kinetics: Table 1). This difference was statistically significant by Fisher's exact testing (positive (%): 31.0% vs. 6.9%, $P < 0.0411$; Table 2), while neither were significantly different to the background rate of detection (positive (%): 17.0% vs. 31.0% $P = 0.0570$ (vaccinated); 14.7% vs. 6.9% $P = 0.2634$ (naturally infected)). Of the 25 epitopes that were

immunoreactive in the vaccinated, nine (31.0%) were also immunoreactive in the naïve, while six (24.0%) were immunoreactive in the vaccinated. This difference was not statistically significant by Fisher's exact test (positive (%): 31.0% vs. 6.9%, $P < 0.5380$; Table 2), while there was a significant increase in the rate of positive epitopes between the background rate of detection and epitopes positive in the naïve and vaccinated (positive (%): 17.0% vs. 36.0% $P = 0.0330$; Table 2), but not in the vaccinated and naturally infected (positive (%): 16.5% vs. 24.0% $P = 0.3965$; Table 2). There was no statistically significant difference between the rates of detection of the six (24.0%) or two (6.9%) of 28 epitopes that were immunoreactive in the naturally infected and immunoreactive in the naïve or vaccinated, respectively (positive (%): 24.0% vs. 6.9%, $P < 0.2516$; Table 1), and no significant difference in these rates of detection when compared to background. There were no epitopes identified that were immunoreactive at all three timepoints. These data demonstrate there was a consistency of epitopes that were immunoreactive between matched donors that were SARS-CoV-2 spike protein naïve and who had been vaccinated.

Given this consistency of epitopes between the naïve and vaccinated donors, we sought to investigate whether the epitopes immunoreactive in donors of various immune statuses were

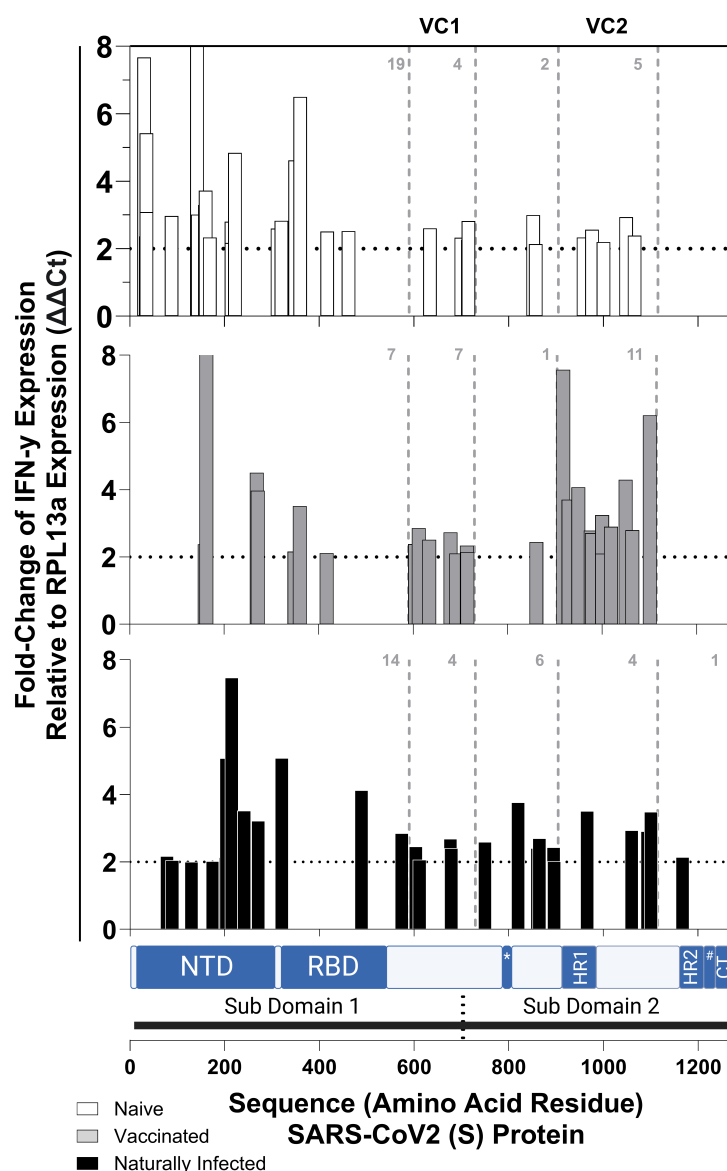


Figure 2. Immunoreactive peptide epitope locations along the SARS-CoV-2 spike (S) protein amino acid sequence. Immunoreactivity was determined as interferon gamma (IFN- γ) expression quantified through a high-throughput RT-qPCR (HTS-RT-qPCR) assay with fold change ($\Delta\Delta C_t$) relative to the endogenous control reference gene Ribosomal Protein L13a (RPL13a) of peripheral blood mononuclear cells (PBMCs) isolated from 12 individuals naïve to SARS-CoV-2 S-protein (naïve; white bars), following homologous AstraZeneca COVID-19 vaccination (vaccinated; grey bars) and following infection with SARS-CoV-2 (naturally infected; black bars) stimulated with 170 SARS-CoV-2 S-protein peptide epitopes. Discrete locations shown along the amino acid sequence are Sub-Domain 1 (1–681) and Sub-Domain 2 (686–1273aa), and the N-terminus (13–304aa; NTD), Receptor Binding (319–541aa; RBD), internal fusion peptide (816–833; *), Heptad Repeat 1 (981–983aa; HR1), Heptad Repeat 2 (1162–1203aa; HR2), transmembrane (1213–1237aa; #), Cytoplasmic Tail (1274 to the end of the protein; CT) domains. Vaccination Cluster 1 (590–730aa; VC1) and Vaccination Cluster 2 (905–1115aa; VC2) were experimentally defined by a high density of immunoreactive epitopes in these regions in donors following vaccination (grey bars). Numbers shown are total immunoreactive ($\Delta\Delta C_t > 2$) epitopes identified within VC1 and VC2 defined regions.

associated with SARS-CoV-2 variant homology. Of the epitopes selected for this study, 38 of 170 (22.3%) had less than 100% homology to all

clinically circulating SARS-CoV-2 variants (Supplementary figure 4), while 8 of 29 (27.6%), 8 of 25 (32.0%) and 10 of 27 (37.0%) peptides that

induced an immunogenic response in the naïve, vaccinated and naturally infected, respectively, did not have 100% homology (Supplementary table 6). There was no significant difference in the number of epitopes with imperfect homology by Fisher's exact testing, either when compared to the total peptides or across donor immune status. These data suggest that 100% epitope sequence homology did not play a significant role in determining epitope immunogenicity.

The localisation of immunoreactive peptide epitopes within the SARS-CoV-2 S-protein is dependent upon immune status

We next sought to determine whether there was variation in the location of immunoreactive epitopes along the SARS-CoV-2 S-protein amino acid sequence amongst donors of either naïve, vaccinated or naturally exposed immune status. Broadly, epitopes appeared to cluster, especially in the vaccinated (Figure 2). This contrasted with the spread of the 170 selected peptide epitopes, which were generally spread across the S-protein sequence (Supplementary figure 2). Fisher's exact testing found there was a statistically significant decrease in the number of immunoreactive epitopes in the N-terminus domain (NTD) following vaccination. Specifically, of the 30 stimulations that were immunoreactive in the naïve, 13 (43.3%) were from peptide epitopes found in the NTD. While of the 26 stimulations identified as immunoreactive following vaccination, only four (15.4%) epitopes were in the NTD (in domain (%): 43.3% vs. 15.4%, $P = 0.0401$; Table 2). There was no significant difference in the number of immunoreactive epitopes in the NTD between the naturally infected and naïve (in domain (%): 34.5% vs. 43.3%; $P = 0.5959$; Table 2) or the naturally infected and vaccinated (in domain (%): 34.5% vs. 15.4%; $P = 0.1302$; Table 2). Furthermore, there were no significant differences in epitope location amongst donors of differing immune status within the receptor-binding domain (Table 2), or any other previously defined tested domains (Supplementary table 7). These data demonstrate that while epitope localisation differed in the vaccinated, it was generally not associated with previously defined domains.

As the immunoreactive epitopes within the vaccinated appeared to generally cluster in two regions (Figure 2), we defined these regions as

Vaccination Cluster 1 (590–730aa; VC1) and Vaccination Cluster 2 (905–1115aa; VC2). Fisher's exact testing found there were no significant differences between the 7 of 26 (26.9%) epitopes located within VC1 that were immunoreactive in the vaccinated compared to the 4 of 30 (13.3%) in the naïve (in domain (%): 26.9% vs. 13.3%; $P = 0.3130$; Table 2) and 4 of 29 (13.8%) in the naturally infected (in domain (%): 26.9% vs. 13.8%; $P = 0.3153$; Table 2). In contrast, the 11 of 26 (42.3%) immunoreactive epitopes in the vaccinated that were located within VC2 were statistically significantly more than the 5 of 30 (16.7%) in the naïve (in domain (%): 42.3% vs. 16.7%; $P = 0.0426$; Table 2) and the 4 of 29 (13.8%) in the naturally infected (in domain (%): 42.3% vs. 13.8%; $P = 0.0321$; Table 2). When combined, 18 of 26 (69.2%) immunoreactive epitopes in the vaccinated were located within either VC1 or VC2, which was statistically significantly more than the 9 of 30 (30.0%) in the naïve (in domain (%): 69.2% vs. 30.0%; $P = 0.0068$; Table 2) and the 8 of 29 (27.6%) in the naturally infected (in domain (%): 69.2% vs. 27.6%; $P = 0.0029$; Table 2). There was no significant difference in the number of immunoreactive epitopes located within VC1, VC2 or when combined between the naïve and naturally infected ($P > 0.9999$ in all cases; Table 2). These data demonstrate that vaccination significantly altered the localisation of immunoreactive epitopes on the SARS-CoV-2 S-protein, causing them to cluster predominantly in two specific regions.

Taken together, this study established that the most immunoreactive epitopes varied following vaccination and subsequent natural infection, shifting from HLA-A in the naïve to HLA-B in the naturally infected. Furthermore, although there was consistency between specific immunoreactive epitopes in naïve and vaccinated donors, vaccination significantly altered the localisation of immunoreactive epitopes, promoting epitopes that clustered within two extra-domainal regions, while subsequent natural infection generally promoted novel epitopes.

DISCUSSION

In this study, we analysed the immunoreactivity of SARS-CoV-2 S-protein peptide epitopes in donors across multiple kinetic timepoints from SARS-CoV-2 S-protein naïve, following AstraZeneca double homologous vaccination, and subsequent natural

exposure to SARS-CoV-2. The results of this study suggested the most immunoreactive SARS-CoV-2 S-protein epitopes varied following vaccination and subsequent natural infection. Immunoreactive epitopes in the naïve were predominantly associated with HLA-A, with nearly half clustering in the N-terminal domain. After vaccination, there was a shift in the localisation of immunoreactive epitopes to two extra-domianial regions. Subsequent natural infection induced novel epitopes that were dispersed across the antigen and primarily associated with HLA-B, specifically the B7 supertype.

The immunoreactivity of SARS-CoV-2 S-protein T-cell epitopes has been extensively studied,^{43,57} and many well-characterised epitopes have been identified as immunoreactive across naïve, vaccinated and naturally infected donors (Supplementary table 3). Nevertheless, herein, we report immunoreactivity in several epitopes in immune status groups for the first time. For example, we report the A*02:01 epitope GLTVLPPLL was immunoreactive in a naïve donor, whereas previously this epitope has only been found to be immunoreactive following natural infection.⁴³ In other epitopes, we report immunoreactivity which is in agreement with some of the literature. For example, we report the A*02:01 epitope VLNDILSRL was immunoreactive in a naïve and vaccinated donor, but we found no immunoreactivity following natural infection. Studies have reported the immunogenicity of VLNDILSRL in naïve individuals,^{58,59} others have not,⁶⁰ while some studies have reported immunogenicity only in naturally infected individuals,³¹ or reported immunogenicity only following certain immunisation strategies.^{44,61} Indeed, many of the epitopes we identified as immunoreactive have inconsistent findings reported in IEDB (Supplementary table 3). Such inconsistencies are frequent in human studies because of the significant environmental and genetic variation inherent in human donors. These inconsistencies may also stem from the influence and interaction of underreported technical variation, such as during PBMC collection, cryopreservation, thawing and culture.⁶² The variation in donor HLA types, available PBMCs and the relatively small sample size (≤ 10 donors per group) of this study is also likely to introduce variability. Larger studies with more uniformly sampled donors would help confirm and expand the observation of this study.

We found there was a statistically significant increase in the number of HLA-B7 supertype epitopes that were immunogenic following natural infection. HLA-B genes have a reported strong association with viral infections,^{63,64} including in COVID-19,⁶⁵ especially the B7 supertype allele HLA-B*15:01, which has been associated with asymptomatic SARS-CoV-2 infections,⁶⁶ and HLA-B*07:02, which is associated with a high degree of pre-existing cross-reactive memory T cells.⁶⁷ Nevertheless, it remains unclear how increasing HLA-B7 allele immunogenicity influences patient outcomes, as HLA-B7 supertype alleles have been associated with increased disease susceptibility.^{68,69} It is also unclear why peptide epitopes associated with HLA-A genes would be prominently immunoreactive in the naïve. There is significant peptide overlap amongst common S-protein epitopes and endogenous tumour-associated epitopes,⁷⁰ which may be activated during healthy immune homeostasis, and core amino acid anchors of epitopes immunoreactive in the naïve have found broad anchor homology in seasonal coronavirus. It remains unclear whether this pre-existing immunity is irrelevant or related to beneficial or detrimental patient outcomes.⁷¹ Our analysis revealed that sequence homology was not correlated with epitope immunogenicity. This finding aligns with existing literature, which indicates that CD4⁺ and CD8⁺ T-cell responses in convalescent COVID-19 patients or recipients of the COVID-19 mRNA vaccines were not significantly impacted by mutations present in SARS-CoV-2 variants.⁷² However, given the tens of thousands of possible epitopes available within the S-protein, more extensive studies are needed to definitively determine the relationship between sequence homology, viral variants, vaccines and epitope immunogenicity.

Our study identified the localisation of immunoreactive epitopes in two extra-domianial regions, between 590–730aa and 905–1115aa of the S-protein following vaccination. Other studies have shown dynamic changes in epitope localisation amongst donors with varying immune statuses. For example, one study found that individuals previously infected with SARS-CoV-2 develop more distinct T-cell immune memory compared to those who are only vaccinated.⁷³ Another study observed that, in naïve patients, both the C- and N-terminal regions of the ORF1 protein contain fewer T-cell epitopes, and in agreement with this study, reported similar

epitope localisation in convalescent and naïve patients.⁶⁰ It is unclear why such localisation of T-cell epitopes would occur in donors of various immune statuses.

The only post-vaccination samples assessed in this study were PBMCs collected from donors following a double homologous AstraZeneca ChAdOx1 nCoV-19 (AZ) vaccination regimen. The AZ vaccine has been found to induce potent CD4⁺ and CD8⁺ T-cell responses.^{74,75} Heterologous boosting with other vaccines, such as the BNT162b2 Pfizer-BioNTech (Pfizer) vaccine, may induce stronger immune responses than a homologous regimen.¹⁸ Investigating the reactivity of peptide epitopes across varying homologous and heterologous vaccine regimens may provide further insight into improving vaccine-induced T-cell immunogenicity against SARS-CoV-2. Post-vaccination and post-infection samples were collected between 1 and 4 months following convalescence, and therefore, the T-cell reactivity observed in this study was more likely associated with long-term immune memory cells.⁷⁶ However, flow-cytometry reactive cell phenotyping would be required to identify which cells are responsible for the immunoreactivity. It is possible that investigating the kinetics of acute phase peptide epitope immunoreactivity and subsequent long-term memory formation may provide insight into the development of long-term cellular immunity.

The *in vivo* development of a T-cell peptide epitope immunodominance hierarchy is a complex process, which remains incompletely understood.⁷⁷ However, several aspects of the formation of immunodominance, such as the relationship between immunogenicity and MHC binding affinity, are relatively well established. Indeed, the binding affinity of peptide epitopes to variable MHC alleles is described as the most selective stage of the formation of an epitope immunodominance hierarchy,³³ and a binding affinity threshold of 500 nM for peptide–MHC interactions has been experimentally established as necessary to initiate T-cell immunity.⁷⁸ We found the Immune Epitope Database (IEDB) HLA-peptide binding score did identify peptide epitopes found to be highly immunoreactive in convalescent COVID-19 patients.⁴³ However, the predictive binding affinity of a putative peptide epitope for a given HLA molecule should not be used as the sole predictor of immunodominance.^{79,80} Variables,

including previous exposure to homologous epitopes, antigen abundance following vaccination and infection, antigen processing, peptide–HLA-binding competition and T-cell receptor (TCR) repertoire, can all influence the immunodominance hierarchy.⁷⁷ We found abundant cross HLA-binding affinities in our prioritised peptide epitopes (Supplementary figure 2). To investigate how the cross-HLA-binding affinities of peptides predicted from the SARS-CoV-2 S-protein impact epitope immunogenicity, a validated immunodominance hierarchy of S-protein epitopes would need to be constructed across variably HLA-matched donors and compared to HLA-peptide binding scores.

Variance in peptide epitope immunogenicity between post-vaccinated and -infected individuals can be partially explained by exposure to viral variants carrying epitope mutations within the S-protein. We found variant-defining mutations crossed several of our peptide epitopes, with the Omicron variant carrying the largest number of S-protein nonsynonymous mutations, mostly within the receptor binding domain (Supplementary figure 3). By late 2023, the most dominant variant circulating globally was Omicron, and due to its global distribution, many sub-variants are now circulating, each with defining mutations.⁸¹ Interestingly, Omicron sub-variants are undergoing convergent evolution, as several areas in the RBD have appeared as mutational hotspots.⁸² While the cause remains unknown, it is likely both humoral and cellular immunity are applying selective pressure to these strains. It is likely that genomic surveillance of viral lineages amongst PBMC donors would provide significant insight into how variants can influence epitope immunogenicity, and how this may relate to the variant evolution.⁸³

In summary, herein we have investigated the immunogenicity of 170 immunodominant peptide epitopes from the S-protein of SARS-CoV-2 in pre-vaccinated, post-vaccinated and post-infected individuals. Our investigation revealed that immunoreactivity was not confined to a select few immunodominant epitopes; instead, it was widely distributed amongst numerous epitopes. Immunoreactive epitopes in the naïve were predominantly associated with HLA-A, which shifted to primary HLA-B following natural infection. Vaccination promoted epitopes that were immunoreactive in the naïve, but primarily within two regions, and natural infection

generally promoted novel epitopes that were dispersed across the S-protein antigen.

METHODS

Peptides

CD8⁺ T-cell epitope prediction and selection

Over 7500 CD8⁺ T-cell peptide epitope–HLA allele combinations with an HLA-binding score > 0.2 were predicted from the S-protein of Wuhan reference strain of SARS-CoV-2 (GenBank: [YP_009724390.1](#)) using the Immune Epitope Database (IEDB) NetMHCpan EL 4.1 algorithm⁴⁹ (Supplementary figure 1). A prioritised list of 145 peptides was defined by sorting epitopes into affinity of binding to HLA-A2, HLA-A3/11, HLA-A24, HLA-B7, and HLA-B8 Class I supertypes, ordering by the sum of the response as reported from Tarke *et al.*⁴³ and, subsequently, the IEDB predicted binding score (Supplementary table 1). Other peptides reported in the literature to be immunoreactive were also included^{21,41,51} (Supplementary table 1).

CD4⁺ T-cell epitope selection

Twenty-five CD4⁺ T-cell S-protein peptide epitopes reported as immunogenic following exposure to SARS-CoV-2 were selected from the literature^{43,46,52} (Supplementary table 1).

In silico predicted CD8⁺ peptide epitope cross-HLA-binding affinity analysis

The capacity of predicted CD8⁺ T-cell peptide epitopes to bind degenerately to multiple HLA alleles (cross-HLA-binding affinity) was determined using the Immune Epitope Database (IEDB) NetMHCpan EL 4.1 algorithm⁴⁹ queried to predict a binding score of each peptide across 27 common alleles within the HLA-A1, A2, A3/11, A24, A3/01, B7, B8, B44, B58 and B62 HLA-supertypes (Supplementary figure 2).

In silico CD4⁺ and CD8⁺ T-cell epitope homology analysis

Variant-defining consensus nonsynonymous mutations in SARS-CoV-2 S-protein relative to the Wuhan consensus sequence were provided by CoVariants⁸⁴ (accessed October 2023) using data from the *Global Initiative on Sharing All Influenza Data* (GISAID). Each peptide (Supplementary figure 3) and the Alpha (B.1.1.7; GenBank: [QWE88920.1](#)), Beta (B.1.351; GenBank: [QRN78347.1](#)), Gamma (B.1.1.28.1; GenBank: [QVE55289.1](#)), Delta (B.1.617.2; GenBank: [QWK65230.1](#)) and Omicron (B.1.1.529; GenBank: [UFO69279.1](#)) strains, and SARS-CoV1 ([YP_009825051.1](#)), MERS (GenBank: [YP_009047204.1](#)), CovNL63 (GenBank: [YP_003767.1](#)), CoV-229E (GenBank: [AAK32191.1](#)), Cov43 (GenBank: [QXL74886.1](#)) and CovHKU1 (GenBank: [YP_173238.1](#)) species of coronavirus were aligned to the SARS-CoV-2 Wuhan strain (GenBank: [YP_009724390.1](#)) using the Multiple Sequence Comparison by

Log-Expectation (MUSCLE; European Bioinformatics Institute) alignment tool with standard settings.⁸⁵

Peptides

T-cell peptide epitopes from SARS-CoV-2 S-protein were synthesised at 95% purity (Mimotopes, Melbourne, Australia) and resuspended in dimethyl sulfoxide (DMSO) at a concentration of 20 mg mL⁻¹.⁸⁶ A positive control CEF peptide pool representing well-characterised CD8⁺ T-cell epitopes from Influenza virus, Epstein–Barr virus and Cytomegalovirus (CEF (HLA Class I Control) Peptide Pool) was purchased commercially (Stem Cell Technologies).

Samples

Ethical approval

This study was performed according to the principles of the Declaration of Helsinki. Ethics approval to undertake the research was obtained from QIMR Berghofer Medical Research Institute Human Research Ethics Committee (HREC: P2282). Informed consent was obtained from all participants. The inclusion criteria for the study were that participants were over the age of 18 and were well and able to donate in adherence with Queensland Health policies. All methods were performed in accordance with institutional guidelines and regulations.

Samples

PBMCs and sera were collected from 11 individuals at three timepoints: (1) Pre-2019 (SARS-CoV-2-naïve), (2) Four weeks post double homologous AstraZeneca™ (ChAdOx1 nCoV-19) vaccination (vaccinated) and (3) 4 weeks post subsequent SARS-CoV-2 infection (naturally infected). Information about which variant each donor was infected with was not available, but the dominant variant circulating during the sampling period was the original Wuhan strain, followed by the Delta and Omicron variants. There were no mortality or severe outcomes (i.e. hospitalisation) during convalescence for all naturally infected donors. Human leukocyte antigen (HLA) typing was performed by AlloSeq Tx17 (CareDx Pty Ltd, Fremantle, Australia) (Supplementary table 2). PBMCs were isolated by standard density gradient centrifugation and cryopreserved in 90% FBS/10% DMSO as previously described.⁵³ PBMCs were thawed at 37°C, rested for 18 h at 2×10^6 cells mL⁻¹ in RPMI-1640 supplemented with 10% heat-inactivated AB human serum (Sigma-Aldrich), 100 U mL⁻¹ penicillin/streptomycin (Thermo Fisher Scientific), 2 mM GlutaMAX (Thermo Fisher Scientific), 10 mM HEPES (Thermo Fisher Scientific) (R10 Media), at 37°C and 10% CO₂.

Detection of SARS-CoV-2 antibodies

Sera were collected from serum-separating tubes following centrifugation as previously described.⁸⁷ Serum antibody titres were analysed on a cobas e411 (Roche Diagnostics) and Abbott Architect i4000SR (Abbott Diagnostics) analyser

using their respective assays as described by the manufacturer. The Abbott SARS-CoV-2 IgG assay detected IgG antibodies to the receptor binding domain (RBD) of the S1 subunit of the S-protein of SARS-CoV-2. The Roche assay detected both IgM and IgG antibodies reactive to the nucleocapsid protein (NCAP) of SARS-CoV-2. Both assays report their respective quantitative signal (QS).

T-cell assays

PBMCs were stimulated in 50 μ L R10 media in 96-well U-bottom plates for 6 h before cells were lysed in MagMAX Lysis Buffer, as previously described.⁵⁶ The number of PBMCs stimulated was normalised across kinetic timepoints but varied between donors ($3.4\text{--}11.5 \times 10^5$ PBMCs/Stimulation; Supplementary table 2). Predicted SARS-CoV-2 T-cell peptides and CEF peptide pool at 2 μ g mL⁻¹ were tested alongside 50 ng mL⁻¹ PMA, 1000 ng mL⁻¹ Ionomycin mitogen positive control and a media-only negative control.

Reverse transcription-quantitative PCR

RNA was extracted and converted to cDNA using our 'High-Throughput Screening (HTS) optimised protocol' as previously described.⁵⁶ Briefly, RNA was isolated using a MagMAX[™] mirVana[™] Total RNA Isolation Kit (Applied Biosystems) and converted to cDNA with SuperScript[™] IV First-Strand Synthesis System (Thermo Fisher) following the manufacturer's instructions, except that all reagents were used at 25% of the volume recommended by the manufacturer, respectively; and the Superscript[™] IV reverse transcriptase enzyme was used at 5 U μ L⁻¹ RNA. Due to the variable numbers of stimulated PBMCs across donors (Supplementary table 2), relative quantification was used for qPCR, as previously described.⁸⁸ Briefly, the fold-change expression of *Interferon gamma* (IFN- γ) were determined relative to the expression of the reference gene *Ribosomal protein L13a* (*RPL13a*). Fold change was normalised relative to the negative control (media only) stimulation. IFN- γ , and *RPL13a* specific desalt-grade (Sigma-Aldrich) previously optimised primers,⁵³ obtained from PrimerBank[™]⁸⁹ were used at 500 nm using ssoAdvanced[™] Universal SYBR[®] Green Master-Mix (Bio-Rad). All reactions were run in technical triplicate in accordance with MIQE guidelines⁸⁸ at 5 μ L total volume with 1 μ L of reverse transcription eluent diluted 1:4 in Ultra-Pure[™] H₂O (Invitrogen). Data were acquired using a QuantStudio5 Real-Time PCR system running QuantStudio Design and Analysis Software (v1.4.3; Applied Biosystems).

Data analysis

To examine the immunoreactivity of peptide epitopes, stimulations were classified as either positive or negative, and these categorical data were tested with Fisher's exact testing. Further categorical data, including epitope homology (Homologous vs. Not Homologous) and immunoreactive epitope localisation (within region vs. outside region), were also tested with a Fisher's exact test.

Kinetic data examining the strength of immunoreactivity of peptide epitopes across donor-matched timepoints were tested with a non-parametric Kruskal–Wallis test, followed by Dunn's corrected multiple comparisons testing. GraphPad Prism version 10.2.0 (GraphPad Software) was used, and in all cases, *P*-values < 0.05 were considered statistically significant.

ACKNOWLEDGMENTS

The researchers thank the study participants. The work was supported by the National Health and Medical Research Council of Australia (NHMRC) grant #1069466 and NHMRC Principal Research Fellowship (#1137285) awarded to DLD. DJB is supported by James Cook University Prestige Research Training Program Stipend (RTPS). The graphical abstract was created with biorender.com. Open access publishing facilitated by The University of Queensland, as part of the Wiley - The University of Queensland agreement via the Council of Australian University Librarians.

CONFLICT OF INTEREST

The authors declare no conflict of interest.

AUTHOR CONTRIBUTIONS

Daniel J Browne: Conceptualization; formal analysis; methodology; writing – original draft; writing – review and editing. **Pauline Crooks:** Methodology; writing – review and editing. **Corey Smith:** Conceptualization; supervision; writing – review and editing. **Denise L Doolan:** Conceptualization; formal analysis; funding acquisition; project administration; supervision; writing – original draft.

DATA AVAILABILITY STATEMENT

The original contributions presented in the study are included in the article and [Supplementary material](#). Further inquiries can be directed to the corresponding author.

REFERENCES

1. Zhou P, Yang XL, Wang XG *et al.* A pneumonia outbreak associated with a new coronavirus of probable bat origin. *Nature* 2020; **579**: 270–273.
2. Arbel R, Peretz A, Sergienko R *et al.* Effectiveness of a bivalent mRNA vaccine booster dose to prevent severe COVID-19 outcomes: a retrospective cohort study. *Lancet Infect Dis* 2023; **23**: 914–921.
3. León TM. COVID-19 cases and hospitalizations by COVID-19 vaccination status and previous COVID-19 diagnosis—California and New York, May–November 2021. *MMWR Morb Mortal Wkly Rep* 2022; **71**: 125–131.
4. Tenforde MW. Effectiveness of mRNA vaccination in preventing COVID-19-associated invasive mechanical ventilation and death—United States, March 2021–January. *MMWR Morb Mortal Wkly Rep* 2022; **71**: 459–465.

5. Olson SM. Effectiveness of Pfizer-BioNTech mRNA vaccination against COVID-19 hospitalization among persons aged 12–18 years—United States, June–September 2021. *MMWR Morb Mortal Wkly Rep* 2021; **70**: 1483–1488.
6. Ferdinands JM. Waning 2-dose and 3-dose effectiveness of mRNA vaccines against COVID-19-associated emergency department and urgent care encounters and hospitalizations among adults during periods of Delta and Omicron variant predominance—VISION Network, 10 states, August 2021–January 2022. *MMWR Morb Mortal Wkly Rep* 2022; **71**: 255–263.
7. Fabiani M, Puopolo M, Morciano C et al. Effectiveness of mRNA vaccines and waning of protection against SARS-CoV-2 infection and severe covid-19 during predominant circulation of the delta variant in Italy: retrospective cohort study. *BMJ* 2022; **376**: e069052.
8. Yarlagaadda H, Patel MA, Gupta V et al. COVID-19 vaccine challenges in developing and developed countries. *Cureus* 2022; **14**: e23951.
9. Tartof SY, Slezak JM, Puzniak L et al. Effectiveness of BNT162b2 BA.4/5 bivalent mRNA vaccine against a range of COVID-19 outcomes in a large health system in the USA: a test-negative case-control study. *Lancet Respir Med* 2023; **11**: 1089–1100.
10. Care AGDoHaA. Childhood immunisation schedule. 2024. https://www.health.qld.gov.au/_data/assets/pdf_file/0032/989114/qld-immunisation-schedule-children.pdf
11. Diseases NCfIaR. Child and adolescent immunization schedule by age. 2024 (Centers for Disease Control and Prevention). <https://www.cdc.gov/vaccines/hcp/imz-schedules/child-adolescent-age.html>
12. Pooley N, Abdool Karim SS, Combadière B et al. Durability of vaccine-induced and natural immunity against COVID-19: a narrative review. *Infect Dis Ther* 2023; **12**: 367–387.
13. Kojima N, Klausner JD. Protective immunity after recovery from SARS-CoV-2 infection. *Lancet Infect Dis* 2022; **22**: 12–14.
14. Shenai MB, Rahme R, Noorchashm H. Equivalency of protection from natural immunity in COVID-19 recovered versus fully vaccinated persons: a systematic review and pooled analysis. *Cureus* 2021; **13**: e19102.
15. Gazit S, Shlezinger R, Perez G et al. The incidence of SARS-CoV-2 reinfection in persons with naturally acquired immunity with and without subsequent receipt of a single dose of BNT162b2 vaccine: a retrospective cohort study. *Ann Intern Med* 2022; **175**: 674–681.
16. Xu K, Fan C, Han Y, Dai L, Gao GF. Immunogenicity, efficacy and safety of COVID-19 vaccines: an update of data published by 31 December 2021. *Int Immunol* 2022; **34**: 595–607.
17. Rose R, Neumann F, Grobe O, Lorentz T, Fickenscher H, Krumbholz A. Humoral immune response after different SARS-CoV-2 vaccination regimens. *BMC Med* 2022; **20**: 31.
18. Barros-Martins J, Hammerschmidt SI, Cossmann A et al. Immune responses against SARS-CoV-2 variants after heterologous and homologous ChAdOx1 nCoV-19/BNT162b2 vaccination. *Nat Med* 2021; **27**: 1525–1529.
19. Yang H, Xie Y, Li C. Understanding the mechanisms for COVID-19 vaccine's protection against infection and severe disease. *Expert Rev Vaccines* 2023; **22**: 186–192.
20. Moss P. The T cell immune response against SARS-CoV-2. *Nat Immunol* 2022; **23**: 186–193.
21. Grifoni A, Sidney J, Vita R et al. SARS-CoV-2 human T cell epitopes: adaptive immune response against COVID-19. *Cell Host Microbe* 2021; **29**: 1076–1092.
22. Sadarangani M, Marchant A, Kollmann TR. Immunological mechanisms of vaccine-induced protection against COVID-19 in humans. *Nat Rev Immunol* 2021; **21**: 475–484.
23. Collins DR, Gaiha GD, Walker BD. CD8⁺ T cells in HIV control, cure and prevention. *Nat Rev Immunol* 2020; **20**: 471–482.
24. Luckheeram RV, Zhou R, Verma AD, Xia B. CD4⁺ T cells: differentiation and functions. *Clin Dev Immunol* 2012; **2012**: 925135.
25. Le Bert N, Tan AT, Kunasegaran K et al. SARS-CoV-2-specific T cell immunity in cases of COVID-19 and SARS, and uninfected controls. *Nature* 2020; **584**: 457–462.
26. Liontos A, Asimakopoulos AG, Markopoulos GS et al. Correlation of lymphocyte subpopulations, clinical features and inflammatory markers during severe COVID-19 onset. *Pathogens* 2023; **12**: 414.
27. Mueller AL, McNamara MS, Sinclair DA. Why does COVID-19 disproportionately affect older people? *Aging* 2020; **12**: 9959–9981.
28. Lerner A, Benzvi C, Vojdani A. HLA-DQ2/8 and COVID-19 in celiac disease: boon or bane. *Microorganisms* 2023; **11**: 2977.
29. Astbury S, Reynolds CJ, Butler DK et al. HLA-DR polymorphism in SARS-CoV-2 infection and susceptibility to symptomatic COVID-19. *Immunology* 2022; **166**: 68–77.
30. Warren RL, Birol I. HLA alleles measured from COVID-19 patient transcriptomes reveal associations with disease prognosis in a New York cohort. *PeerJ* 2021; **9**: e12368.
31. Habel JR, Nguyen THO, van de Sandt CE et al. Suboptimal SARS-CoV-2-specific CD8⁺ T cell response associated with the prominent HLA-A*02:01 phenotype. *Proc Natl Acad Sci USA* 2020; **117**: 24384–24391.
32. Frelinger JA. *Immunodominance: The Choice of the Immune System*. Hoboken, NJ: John Wiley & Sons; 2006.
33. Yewdell JW, Bennink JR. Immunodominance in major histocompatibility complex class 1 restricted T lymphocyte responses. *Annu Rev Immunol* 1999; **17**: 51–88.
34. Dendrou CA, Petersen J, Rossjohn J, Fugger L. HLA variation and disease. *Nat Rev Immunol* 2018; **18**: 325–339.
35. Almehdi AM, Khoder G, Alchakee AS, Alsayyid AT, Sarg NH, Soliman SSM. SARS-CoV-2 spike protein: pathogenesis, vaccines, and potential therapies. *Infection* 2021; **49**: 855–876.
36. Schetelig J, Heidenreich F, Baldauf H et al. Individual HLA-A, -B, -C, and -DRB1 genotypes are no major factors which determine COVID-19 severity. *Front Immunol* 2021; **12**: 698193.
37. Folegatti PM, Ewer KJ, Aley PK et al. Safety and immunogenicity of the ChAdOx1 nCoV-19 vaccine against SARS-CoV-2: a preliminary report of a phase 1/2, single-blind, randomised controlled trial. *Lancet* 2020; **396**: 467–478.

38. Jackson LA, Anderson EJ, Rouphael NG et al. An mRNA vaccine against SARS-CoV-2—preliminary report. *N Engl J Med* 2020; **383**: 1920–1931.
39. Sahin U, Muik A, Derhovanessian E et al. COVID-19 vaccine BNT162b1 elicits human antibody and TH1 T cell responses. *Nature* 2020; **586**: 594–599.
40. Peng Y, Mentzer AJ, Liu G et al. Broad and strong memory CD4⁺ and CD8⁺ T cells induced by SARS-CoV-2 in UK convalescent individuals following COVID-19. *Nat Commun* 2020; **21**: 1336–1345.
41. Grifoni A, Weiskopf D, Ramirez SI et al. Targets of T cell responses to SARS-CoV-2 coronavirus in humans with COVID-19 disease and unexposed individuals. *Cell* 2020; **181**: 1489–1501.
42. Ferretti AP, Kula T, Wang Y et al. Unbiased screens show CD8⁺ T cells of COVID-19 patients recognize shared epitopes in SARS-CoV-2 that largely reside outside the spike protein. *Immunity* 2020; **53**: 1095–1107.
43. Tarke A, Sidney J, Kidd CK et al. Comprehensive analysis of T cell immunodominance and immunoprevalence of SARS-CoV-2 epitopes in COVID-19 cases. *Cell Rep Med* 2021; **2**: 100204.
44. Tarke A, Coelho CH, Zhang Z et al. SARS-CoV-2 vaccination induces immunological T cell memory able to cross-recognize variants from Alpha to Omicron. *Cell* 2022; **185**: 847–859.
45. Naranbhai V, Nathan A, Kaseke C et al. T cell reactivity to the SARS-CoV-2 Omicron variant is preserved in most but not all individuals. *Cell* 2022; **185**: 1041–1051.
46. Kundu R, Narean JS, Wang L et al. Cross-reactive memory T cells associate with protection against SARS-CoV-2 infection in COVID-19 contacts. *Nat Commun* 2022; **13**: 80.
47. Wang G, Xiang Z, Wang W, Chen Z. Seasonal coronaviruses and SARS-CoV-2: effects of preexisting immunity during the COVID-19 pandemic. *J Zhejiang Univ Sci B* 2022; **23**: 451–460.
48. Young HA, Hodge DL. Interferon- γ . In: Henry HL, Norman AW, eds. *Encyclopedia of Hormones*. New York, NY: Academic Press; 2003:391–397.
49. Reynisson B, Alvarez B, Paul S, Peters B, Nielsen M. NetMHCpan-4.1 and NetMHCIIpan-4.0: improved predictions of MHC antigen presentation by concurrent motif deconvolution and integration of MS MHC eluted ligand data. *Nucleic Acids Res* 2020; **48**: 449–454.
50. Vita R, Mahajan S, Overton JA et al. The immune epitope database (IEDB): 2018 update. *Nucleic Acids Res* 2019; **47**: 339–343.
51. Zhang Z, Mateus J, Coelho CH et al. Humoral and cellular immune memory to four COVID-19 vaccines. *Cell* 2022; **185**: 2434–2451.
52. Sette A, Sidney J, Crotty S. T cell responses to SARS-CoV-2. *Annu Rev Immunol* 2023; **41**: 343–373.
53. Browne DJ, Brady JL, Waardenberg AJ, Loiseau C, Doolan DL. An analytically and diagnostically sensitive RNA extraction and RT-qPCR protocol for peripheral blood mononuclear cells. *Front Immunol* 2020; **11**: 402.
54. Ashoor I, Najafian N, Korin Y et al. Standardization and cross validation of alloreactive IFN γ ELISPOT assays within the clinical trials in organ transplantation consortium. *Am J Transplant* 2013; **13**: 1871–1879.
55. Trauet J, Bourgoin P, Schuldt J et al. Studying antigen-specific T cells through a streamlined, whole blood-based extracellular approach. *Cytometry A* 2024; **105**: 288–296.
56. Browne DJ, Kelly AM, Brady JL, Doolan DL. A high-throughput screening RT-qPCR assay for quantifying surrogate markers of immunity from PBMCs. *Front Immunol* 2022; **13**: 962220.
57. Jin X, Liu X, Shen C. A systemic review of T-cell epitopes defined from the proteome of SARS-CoV-2. *Virus Res* 2023; **324**: 199024.
58. Prakash S, Srivastava R, Coulon PG et al. Genome-wide B cell, CD4⁺, and CD8⁺ T cell epitopes that are highly conserved between human and animal coronaviruses, identified from SARS-CoV-2 as targets for preemptive pan-coronavirus vaccines. *J Immunol* 2021; **206**: 2566–2582.
59. Lv Y, Ruan Z, Wang L, Ni B, Wu Y. Identification of a novel conserved HLA-A*0201-restricted epitope from the spike protein of SARS-CoV. *BMC Immunol* 2009; **10**: 61.
60. Saini SK, Hersby DS, Tamhane T et al. SARS-CoV-2 genome-wide T cell epitope mapping reveals immunodominance and substantial CD8⁺ T cell activation in COVID-19 patients. *Sci Immunol* 2021; **6**: eabf7550.
61. Xiao C, Ren Z, Zhang B et al. Insufficient epitope-specific T cell clones are responsible for impaired cellular immunity to inactivated SARS-CoV-2 vaccine in older adults. *Nat Aging* 2023; **3**: 418–435.
62. Browne DJ, Miller CM, Doolan DL. Technical pitfalls when collecting, cryopreserving, thawing, and stimulating human T-cells. *Front Immunol* 2024; **15**: 1382192.
63. Martin MP, Carrington M. Immunogenetics of HIV disease. *Immunol Rev* 2013; **254**: 245–264.
64. Singh R, Kaul R, Kaul A, Khan K. A comparative review of HLA associations with hepatitis B and C viral infections across global populations. *World J Gastroenterol* 2007; **13**: 1770–1787.
65. Peng Y, Felce SL, Dong D et al. An immunodominant NP105–113-B*07:02 cytotoxic T cell response controls viral replication and is associated with less severe COVID-19 disease. *Nat Immunol* 2022; **23**: 50–61.
66. Augusto DG, Murolo LD, Chatzileontiadou DSM et al. A common allele of HLA is associated with asymptomatic SARS-CoV-2 infection. *Nature* 2023; **620**: 128–136.
67. Francis JM, Leistritz-Edwards D, Dunn A et al. Allelic variation in class I HLA determines CD8⁺ T cell repertoire shape and cross-reactive memory responses to SARS-CoV-2. *Sci Immunol* 2022; **7**: eabk3070.
68. Ng MH, Lau KM, Li L et al. Association of human-leukocyte-antigen class I (B*0703) and class II (DRB1*0301) genotypes with susceptibility and resistance to the development of severe acute respiratory syndrome. *J Infect Dis* 2004; **190**: 515–518.
69. Sanchez-Mazas A. HLA studies in the context of coronavirus outbreaks. *Swiss Med Wkly* 2020; **150**: 20248.
70. Kanduc D. From anti-severe acute respiratory syndrome coronavirus 2 immune response to cancer onset via molecular mimicry and cross-reactivity. *Glob Med Genet* 2021; **8**: 176–182.

71. Sette A, Crotty S. Pre-existing immunity to SARS-CoV-2: the knowns and unknowns. *Nat Rev Immunol* 2020; **20**: 457–458.
72. Tarke A, Sidney J, Methot N *et al.* Impact of SARS-CoV-2 variants on the total CD4⁺ and CD8⁺ T cell reactivity in infected or vaccinated individuals. *Cell Rep Med* 2021; **20**: 100355.
73. Rodda LB, Morawski PA, Pruner KB *et al.* Imprinted SARS-CoV-2-specific memory lymphocytes define hybrid immunity. *Cell* 2022; **185**: 1588–1601.
74. Deming ME, Lyke KE. A 'mix and match' approach to SARS-CoV-2 vaccination. *Nat Med* 2021; **27**: 1510–1511.
75. Swanson PA, Padilla M, Hoyland W *et al.* AZD1222/ChAdOx1 nCoV-19 vaccination induces a polyfunctional spike protein-specific TH1 response with a diverse TCR repertoire. *Sci Transl Med* 2021; **17**: eabj7211.
76. Cox RJ, Brokstad KA. Not just antibodies: B cells and T cells mediate immunity to COVID-19. *Nat Rev Immunol* 2020; **20**: 581–582.
77. Yewdell JW. MHC class I immunopeptidome: past, present, and future. *Mol Cell Proteomics* 2022; **21**: 100230.
78. Sette A, Vitiello A, Rehman B *et al.* The relationship between class I binding affinity and immunogenicity of potential cytotoxic T cell epitopes. *J Immunol* 1994; **153**: 5586–5592.
79. Bihl F, Frahm N, Di Giammarino L *et al.* Impact of HLA-B alleles, epitope binding affinity, functional avidity, and viral coinfection on the immunodominance of virus-specific CTL responses. *J Immunol* 2006; **176**: 4094–4101.
80. Yang X, Zhao L, Wei F, Li J. DeepNetBim: deep learning model for predicting HLA-epitope interactions based on network analysis by harnessing binding and immunogenicity information. *BMC Bioinformatics* 2021; **22**: 231.
81. Roemer C, Sheward DJ, Hisner R *et al.* SARS-CoV-2 evolution in the Omicron era. *Nat Microbiol* 2023; **8**: 1952–1959.
82. Cao Y, Jian F, Wang J *et al.* Imprinted SARS-CoV-2 humoral immunity induces convergent Omicron RBD evolution. *Nature* 2023; **614**: 521–529.
83. Merhi G, Koweyes J, Salloum T, Khoury CA, Haidar S, Tokajian S. SARS-CoV-2 genomic epidemiology: data and sequencing infrastructure. *Future Microbiol* 2022; **17**: 1001–1007.
84. Hodcroft EB. Covariants: SARS-CoV-2 mutations and variants of interest. 2021. <https://covariants.org/>
85. Edgar RC. MUSCLE: multiple sequence alignment with high accuracy and high throughput. *Nucleic Acids Res* 2004; **32**: 1792–1797.
86. Currier JR, Kuta EG, Turk E *et al.* A panel of MHC class I restricted viral peptides for use as a quality control for vaccine trial ELISPOT assays. *J Immunol Methods* 2002; **260**: 157–172.
87. Body A, Lal L, Srihari S *et al.* Comprehensive humoral and cellular immune responses to COVID-19 vaccination in adults with cancer. *Vaccine* 2025; **46**: 126547.
88. Bustin SA, Benes V, Garson JA *et al.* The MIQE guidelines: minimum information for publication of quantitative real-time PCR experiments. *Clin Chem* 2009; **55**: 611–622.
89. Spandidos A, Wang X, Wang H, Seed B. PrimerBank: a resource of human and mouse PCR primer pairs for gene expression detection and quantification. *Nucleic Acids Res* 2010; **38**: 792–799.

Supporting Information

Additional supporting information may be found online in the Supporting Information section at the end of the article.



This is an open access article under the terms of the [Creative Commons Attribution](#) License, which permits use, distribution and reproduction in any medium, provided the original work is properly cited.